

Research Article

Aditya Rio Prabowo*, Ridwan Ridwan, Moritz Braun, Shi Song, Sören Ehlers, Nurman Firdaus, and Ristiyanto Adiputra

Comparative study of shell element formulations as NLFE parameters to forecast structural crashworthiness

<https://doi.org/10.1515/cls-2022-0217>

received October 16, 2022; accepted September 06, 2023

Abstract: This work made a comparison of the effects of selected element formulations (EFs) through nonlinear finite element analysis (NLFEA) and physical configurations in scenario design, particularly target locations. The combined results help in quantifying structural performance, focusing on crashworthiness criteria. The analysis involves nonlinear dynamic finite element methods, using an explicit approach applied to an idealized system. This system models ship-to-ship collisions, specifically the interaction between Ro and Ro and cargo reefer vessels, with one striking the other. Summarizing initial NLFEA results reveals that the chosen EF significantly influences the crashworthiness criteria. Notably, differences in formulations lead to different calculation times. The Belytschko–Tsay (BT) EF is the quickest, followed by the Belytschko–Leviathan (BL), with around a 36% difference. Conversely, formulations such as the Hughes–Liu involve much longer processing times, more than twice that of BT. To address the potential impact of shear locking and hourglassing on calculation accuracy during impact, the fully integrated (FI) version of the EF is used. It mitigates these undesired events. For formulations with the same approach, the FI BT formulation suppresses hourglassing effectively, unlike others that show orthogonal hourglassing increments. To ensure reliability, rules were set to assess hourglassing. The criterion is that the ratio of hourglass energy to internal energy should be $\leq 10\%$. All formulations meet this criterion and are suitable as geometric models in NLFEA. Regarding reliability and processing time, analyzing the computation time offers insights. Based on calculations, BL is the fastest, followed by Belytschko–Wong–Chiang, while the FI BT formulation takes more time for the same collision case.

* **Corresponding author: Aditya Rio Prabowo**, Department of Mechanical Engineering, Universitas Sebelas Maret, Surakarta 57126, Indonesia, e-mail: aditya@ft.uns.ac.id

Keywords: structural performance, ship–ship collision, nonlinear finite element analysis, element formulation, crashworthiness criteria

1 Introduction

The potential for massive casualties involved following maritime accidents, *e.g.*, collision, grounding, and explosion, means that impact loading must be considered to avoid fatalities [1–5]. Estimation of the structural performance when subjected to this loading type has developed since the first damage energy formula was introduced by Minorsky [6], and refined versions of this formula have been presented by Woisin [7], Vaughan [8], and Zhang *et al.* [9]. Various studies have followed this finding, *i.e.*, through the improved estimation obtained by including data from analytical analyses [10,11] and laboratory experiments [12,13]. On the other hand, the rapid development of computational technology that took place in the late 1990s provided the finite element (FE) approach as one alternative calculation method for structural investigation, especially for modeling delicate subjects and characteristics. An advantage of this methodology is the reduced risk of time loss due to rejection or failure, which is the main reason that engineering phenomena are suitable to be idealized

Ridwan Ridwan: Department of Mechanical Engineering, Universitas Merdeka Madiun, Madiun 63133, Indonesia

Moritz Braun: Institute of Maritime Energy Systems, German Aerospace Center (DLR), Geesthacht 21502, Germany

Shi Song: Institute for Ship Structural Design and Analysis, Hamburg University of Technology, Hamburg 21073, Germany

Sören Ehlers: Institute of Maritime Energy Systems, German Aerospace Center (DLR), Geesthacht 21502, Germany; Institute for Ship Structural Design and Analysis, Hamburg University of Technology, Hamburg 21073, Germany

Nurman Firdaus, Ristiyanto Adiputra: Research Center for Hydrodynamics Technology, National Research and Innovation Agency (BRIN), Surabaya 60112, Indonesia

using the FE approach. Nevertheless, considering the complexity of the nonlinear behavior of materials and time dependency during impact, a detailed definition of the material and other parameters in terms of the geometry and boundary conditions needs to be developed using the nonlinear finite element analysis (NLFEA) [14–17].

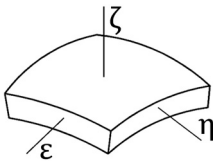
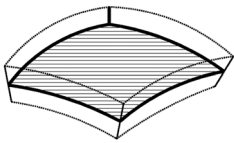
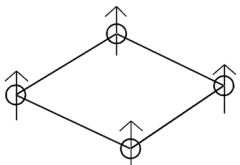
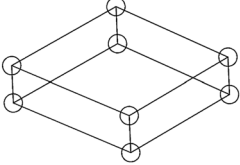
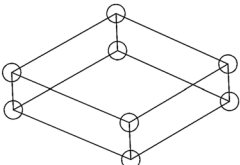
Designs of impact loading for application in maritime accident investigation are created by considering physical parameters, *e.g.*, impact speed, interaction angle, vessel mass, and target location, which involve model idealization and assumption, *i.e.*, calculation parameters in NLFEA, which inevitably lead to diverging results; proper quantification is required to control the validity of the method. One of the fundamental parameters is element formulation (EF), which has to be defined in every FE calculation. This formulation is embedded in the geometrical model (marine vessels are mostly assumed to be thin-walled structures [18–20]), which directly contributes to the magnitudes and contours of structural performance. Although its importance influences the result estimation, the formulation has not been widely discussed as studies related to this subject are scant.

In the realm of engineering, finite element analysis (FEA) has proven to be an invaluable tool for simulating and understanding the complex behaviors of materials and structures. This methodology allows engineers to assess

the performance of various systems under different conditions, aiding in the design, analysis, and optimization of structures subjected to diverse loads. However, the nonlinear behavior of materials and the temporal aspect of progressive phenomena, especially during impact scenarios, pose significant challenges that demand a refined approach. In this review, we delve into the advantages and challenges of using NLFEA for investigating maritime accidents, with an emphasis on the impact loading dynamics.

This study aimed to undertake a comparison of a series of impact loading scenarios, each grounded in a geometrical assumption. These scenarios will be calculated using NLFEA in order to assess the influence of EF on the resulting outcomes. The initial phase involves benchmarking against pioneer laboratory experiments and an established shell formulation. The primary objectives here are to validate the reliability of the current NLFEA methodology and make preliminary predictions regarding the effects of different formulation types on the structural performance. Subsequently, an expanded investigation will be conducted. This phase will involve a modeled double-hull passenger vessel subjected to ship–ship collision conditions. The assessment will consider performance criteria, such as energy, effective strain, and displacement, to precisely quantify how the chosen shell EF impacts the structural response of the ship under impact loading conditions.

Table 1: Thin-walled structure characteristics

Original form	Method	Definition process
 <p>3D shell body (continuous)</p>	<p>Shell</p> <p>Reduction into 2D (semi-discretization <i>e.g.</i>, linear in ζ)</p>	 <p>Shell model (discrete in ζ, continuous in $\xi \eta$)</p> <p>FE discretization 2D shape functions (<i>e.g.</i>, bilinear in $\xi \eta$)</p>  <p>6 degrees of freedom (DOF) per node, <i>e.g.</i>, 4 nodes per element</p>
	<p>Solid</p> <p>FE discretization 3D shape functions (<i>e.g.</i>, trilinear in $\xi \eta \zeta$)</p>	 <p>3 DOF per node, <i>e.g.</i>, 8 nodes per element</p>
	<p>Solid shell</p> <p>Special EF, <i>e.g.</i>, assumed strain formulation</p>	

2 Shell formulation and theory

The application of a shell element in idealizing thin-walled structures using the FE approach has conventionally occurred due to hardware limitations and efficiency of analysis. Thin-walled structures in the real world are one type of three-dimensional shell body, which can be modeled *via* three different methodologies, as presented in Table 1. Implementation of the shell method, a component of shell formulation, requires good understanding. The evolution of shell models began with the Kirchhoff–Love theory regarding membrane and bending effects, which was introduced in 1888; two points are underlined as the main topic, *i.e.*, membrane and bending action and inextensible deformations [21]. The fundamental assumption of this theory is that the cross sections remain straight, unstretched, and normal to mid-surface. Contradiction occurred and required a modification of the material law when stress σ_{zz} and ε_{zz} remain zero. The next idea, proposed in the middle of the 20th century, the Reissner–Mindlin–Naghdi theory, proposed transverse shear strain. This theory excluded a criterion of the previous theory, *i.e.*, cross sections normal to mid-surface [22]. Nevertheless, the weaknesses of the Kirchhoff–Love theory had not been solved. The Ahmad–Iron–Zienkiewicz theory from 1968 introduced a concept, the so-called degenerated solid approach, in which shell theory is defined as semidiscretization of a 3D continuum [23]. After 1990, the widely used assumption was 3D-shell FEs, solid shells, and surface-oriented (continuum shell) elements [24–26].

The derivation of these theories' evolution is implemented in FE calculation in the form of shell EF, which must be defined. Several formulations embedded in ANSYS

LS-DYNA are described in Table 2, including Belytschko–Tsay (BT) (default), Belytschko–Wong–Chiang (BWC), Belytschko–Leviathan (BL), and fully integrated (FI) BT [28–31].

In recent years, there has been growing interest in the analysis of shell structures based on higher-order theories that can account for the dynamic effects and layer-wise (LW) variation of the field variables [32–35]. Among these theories are the LW approach, the equivalent single-layer (ESL) approach, and the equivalent layer-wise (ELW) approach. Some examples of these theories are the generalized higher-order LW theory for the dynamic study of anisotropic doubly curved shells with a mapped geometry; an ELW approach for the free vibration analysis of thick and thin laminated and sandwich shells; and LW and ESL models for smart multi-layered plates.

3 FE benchmarking

Benchmarking in FEA is the process of comparing the performance and accuracy of different numerical models of a physical system. A benchmark FE model is a reliable model that can fully and correctly reflect the real behavior of the structure and has been verified by field tests. It is also important for validating the assumptions and approximations made in the finite EF, such as the material properties, the boundary conditions, and the mesh size, as well as for identifying the strengths and weaknesses of different methods, such as linear or nonlinear, static or dynamic, and implicit or explicit. Benchmarking can also help to establish best practices and standards for FEA in various fields related to engineering and applied mathematics.

Table 2: General options of shell formulations

EF	Characteristics
BT (KEYOPT(1) = 0 or 2) – default	<ul style="list-style-type: none"> • Very fast and recommended for most applications • Uses reduced integration (one point)
BWC (KEYOPT(1) = 10)	<ul style="list-style-type: none"> • Should not be used when elements experience excessive warping [27] • 25% slower than BT • Uses reduced integration (one point)
BL (KEYOPT(1) = 8)	<ul style="list-style-type: none"> • Generally gives correct results for warping • 40% slower than BT
FI BT (KEYOPT(1) = 12)	<ul style="list-style-type: none"> • Reduced integration formulation (one point) • Includes physical hourglass control automatically • 2.5 times slower than reduced integration BT shell • Has four integration points in plane and does not need hourglass control • Shear locking is remedied by assumed strain for the transverse shear • Recommended if hourglass modes are a problem in the analysis

3.1 Configuration and setting

Benchmarking is conducted in the initial stage of this study to validate the current FEA methodology. The laboratory test performed by Alsos and Amdahl [36] is taken as a reference, with the results of this work compared to theirs. The test, which used a scaled model of a medium-sized tanker structure, is idealized numerically in FEA using ANSYS LS-DYNA with a plate panel loaded laterally by a rigid indenter until material fracture or failure occurred. The location of the contact between the plate and the indenter is the center of the plate with a size of $720 \times 1,200 \times 5$ mm. The panel consists of two main parts applied by different materials, *i.e.*, plate and hollow frame. The plate is embedded by steel-grade S235JR-EN10025 with a yield strength of 285 MPa, a hardening coefficient of 0.24, and a failure strain of 0.35. On the other hand, steel S235JR-EN10210 is set on the frame with a yield strength of 390 MPa, a hardening coefficient of 0.18, and a failure strain of 0.28.

The FE analysis time was stopped 0.55 s after the initial movement of the indenter, while the friction coefficient was set based on the Coulomb coefficient values in the range of 0.1–0.3. The lateral displacement of the indenter was idealized by embedding uniform velocity on it with a value of 0.6 m/s. The velocity input was generated and matched with the time simulation to produce the same final displacement results, as shown in the laboratory tests, which used a displacement control of 10 mm/min.

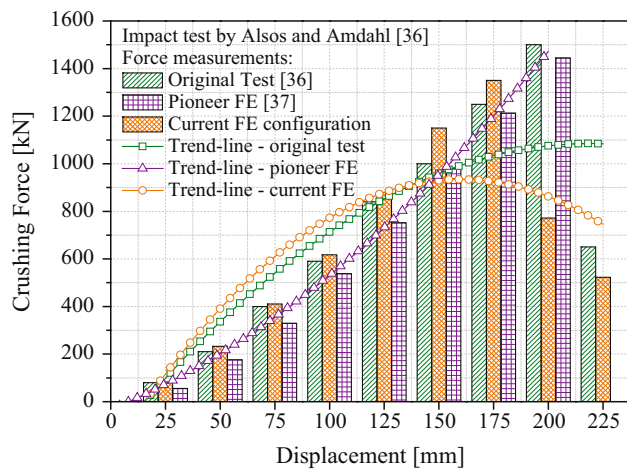


Figure 1: Comparison of the test by Alsos and Amdahl [36] with the pioneering work in FEA by Cerik *et al.* [37].

3.2 Benchmarking results

The obtained results for crushing force in Figure 1 indicate that the current methodology produced good similarity. Both results displayed increment tendency with a maximum state recorded in the range of 175–200 mm; after this point, the force was reduced as a fracture occurred on the target plate. The setting of material characteristics, *i.e.*, fracture/failure criteria, is also compared in this discussion, and a recent work by Cerik *et al.* [37], who proposed the Hosford–Coulomb criterion for shell structures, is considered.

The comparison shows the correspondence of the current work with the original test and a pioneering FE analysis in which the maximum state was reached at 175–200 mm, but the results of the study by Cerik *et al.* [37] showed early analysis termination as no response was recorded at a displacement of 225 mm. A variation in mesh size is considered a major influence in FE analysis and requires calibration to obtain satisfying results. The tendency in Figure 2 illustrates that in terms of fracture occurrence (indicated by the maximum state of force), the mesh size of 15 mm in the current work is the closest to the results using the Hosford–Coulomb criterion [38–40] with a displacement of 200 mm. There is also similarity of these results in terms of the fracture pattern, as shown in Figure 3, which reveals that crescent-moon-like tearing took place during the impact on the plate panel. Based on benchmarking using laboratory tests [36] to validate the reliability of reproducing the actual test/

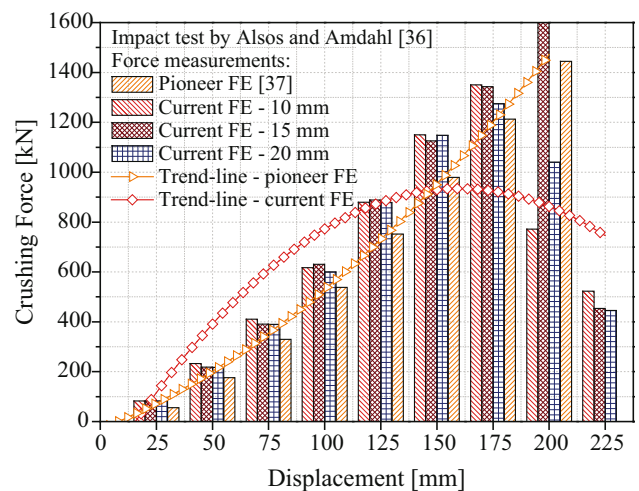


Figure 2: Influence of mesh size on crushing force, accounting for the variety of shell formulations.

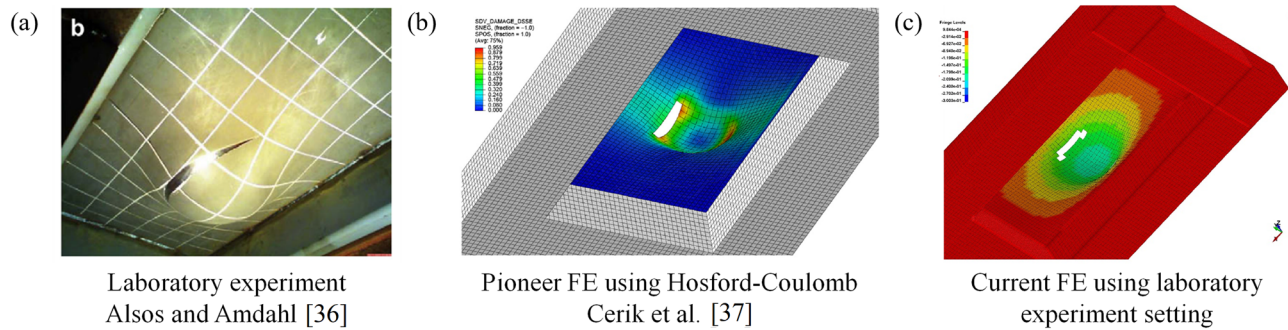


Figure 3: Structural contours of the test that compared the pioneering work and the current work to calibrate fracture behaviors: (a) laboratory experiment using Alsos and Amdahl [36], (b) pioneer FE using Hosford-Coulomb Cerik *et al.* [37], and (c) current FE using laboratory experiment setting.

phenomenon, and FE simulation [37] to verify material fracture characteristic in this stage, the satisfactory nature of the current FE methodology was confirmed.

4 Methodology and analysis preparation

An extended study is performed in the following section to assess the responses of larger structures, *i.e.*, ships. Ship–ship collision is assumed as the main scenario and involves a double-hull passenger ship as the target ship and a cargo ship as the striking ship. Regardless, a previous study has shown that ship–ship collision can be prevented using radar, but the fact is that these severe accidents still happen all over the world [41]. The target ship is idealized in FE analysis to have deformable thin-walled structures [42–45], with three regions set to apply proper mesh sizes. The smallest size, 8–9 mm, was applied to the core region, which was expected to experience the direct impact of the striking ship, with major deformation expected to occur. The 9–10 mm element size was embedded on the transition region as a hub between the core and the outermost regions. A larger size with size 10 mm and above was implemented in the outermost zone as it is predicted that no fracture will occur or expand into this region. The striking ship, on the other hand, is designed as a rigid structure, which means that all the absorbed/internal energy in the collision is focused on the target ship. The striking ship is given a uniform velocity, approaching the targets at 15 kts or approximately 7.72 m/s. As impact occurs between the two ships, the contact model must be defined with the impact that was modeled by automatic contact and the friction coefficient between steels implemented.

The conditions of the impact were dominated by the movement of the striking ship, while the target ship was restrained for its axial and rotational displacement at its original location. The fixation was applied at the ends of the deformable structure, including web frames and bottom members. The schematic illustration presented in Figure 4 indicates the three vertical locations on the target ship selected as impact points for the striking ship. Fundamentally, these points were determined based on the possible increase in the striking ship’s draught. Precisely, these were located on the middle deck (approx. 9 m from the baseline (BL)), side shell (approx. 10 m from the BL), and main deck (approx. 11 m from the BL) and labeled Points 1–3, respectively. In order to quantify the effect of EF on crashworthiness criteria and time processing, the structures were applied by four augmented shell EFs: the BT EF = 0, the BL (EF = 8), the BWC (EF = 10), and the FI version of the BT (EF = 12) [28,29].

5 Extended study of structural crashworthiness

The physical configuration in scenario design refers to the arrangement of the target locations that are subjected to impact loading. The target locations can be chosen based on the expected collision scenarios or the critical regions of the ship structure. The results of the combined parameters, such as EF, material model, and physical configuration, are assessed to quantify structural performance under impact loading. Structural performance can be measured by various crashworthiness criteria, such as energy absorption, which is the amount of kinetic energy lost by the structure during deformation; effective strain, which is a measure of the average plastic deformation in a region of interest;

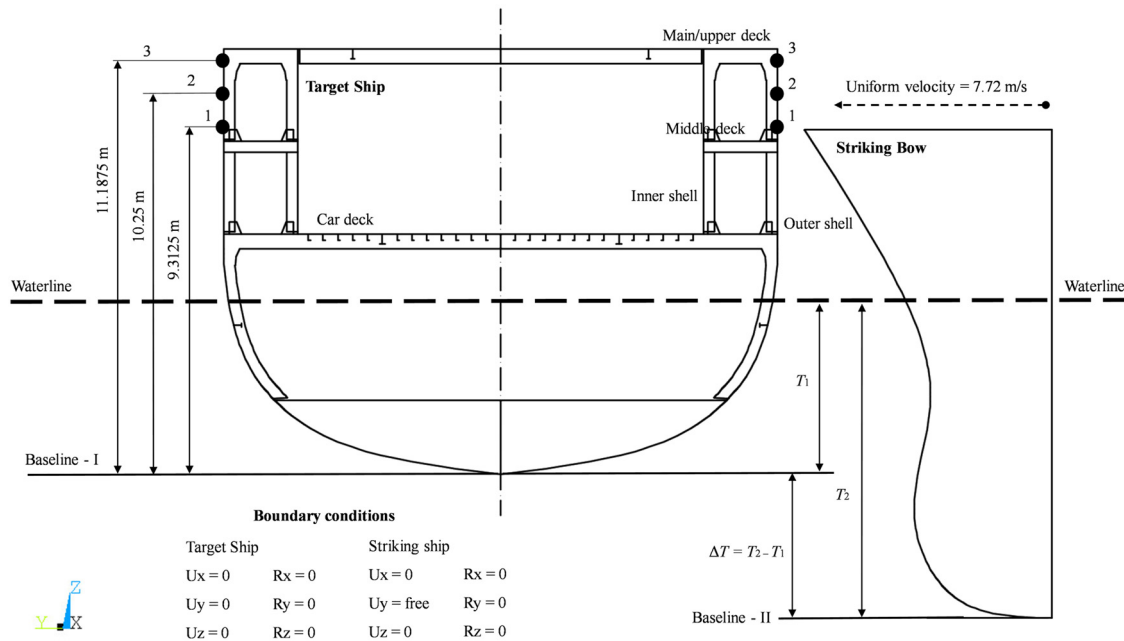


Figure 4: Designed collision scenario for the extended study of formulation influence on crashworthy structures.

displacement, which is the change in position or shape of the structure due to loading; and damage extent, which is the size and location of cracks or fractures in the structure. These criteria can indicate the level of deformation, fracture, and failure of the ship structure due to impact loading.

5.1 Internal energy and crushing force

During impact, the involved structures produce a response in the form of energy as a consequence of the destroyed or deformed members. This energy type is called internal energy or absorbed energy in the literature related to crashworthiness [46–48]. The results displayed in Table 3 indicate that quite a different energy level is shown by the BL formulation, with an estimate of 13% compared to the highest energy produced by the BT formulation. Kinetic

energy is another energy response that expresses the movement of the involved parameters. The overall tendency to give a prediction of higher internal energy is caused by higher kinetic energy. A change in the hourglass energy reflects irregularities during the structure's deformation and ultimate destruction. Lower hourglass energy is desired in the analysis, especially in NLFEA. The FI version of the BT is proven to be the most powerful formulation that is capable of fully suppressing this energy. The total energy is the sum of all energy types in the collision process. An assessment is conducted on internal energy, kinetic energy, hourglass energy, and total energy and finds that other energy, in the range of 14–17%, also contributes to the process. This energy is defined in the FE analysis as contact (sliding) energy, rigid wall energy, and system damping energy. Overall assessment in terms of energy shows good similarity between all the selected formulations, of which the BL is noted as the formulation that

Table 3: Energy results of the selected shell formulations

Formulation	Kinetic K (J)	Internal I (J)	Hourglass H (J)	Total T (J)	I/K Ratio (-)	H/I Ratio (-)	$I + K + H$ (-)	$(I + K + H)/T$ (-)	$(I + K)/T$ (-)	Other energy (-)
BL	1,492,730	5,982,160	148,742	9,233,940	0.2495	0.0996	7,623,632	0.8256	0.8095	0.1744
BT	2,204,380	6,875,120	493,751	12,105,200	0.3206	0.2240	9,573,251	0.7908	0.7500	0.2092
BT-FI	1,425,950	6,787,900	0	10,148,000	0.2101	0	8,213,850	0.8094	0.8094	0.1906
BWC	1,475,710	6,815,060	389,818	10,210,200	0.2165	0.2642	8,680,588	0.8502	0.8120	0.1498

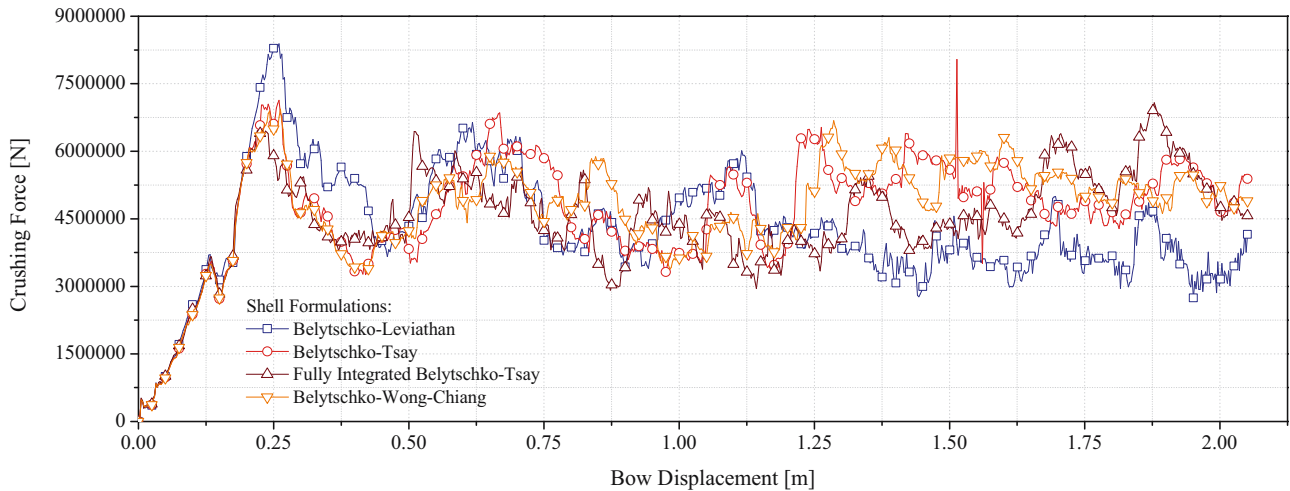


Figure 5: Tendency of the crushing force during ship–ship collision.

underestimated internal energy compared to the others. On the other hand, the reliability of NLFEA was successfully guaranteed by the FI version of BT, followed by BL with the lowest value for the hourglass energy/internal energy ratio.

The crushing force is the acting force at the moment the deformable structure experiences a fracture and the latter is destroyed. The tendency in Figure 5 is very similar until bow displacement at 0.25 m, when it can be predicted that a major fracture of the target ship has not been manifested. After this displacement distance, the BL formulation shows a higher response, while for the BT, the FI version of BT, and the BWC, it takes place approximately until the end of the collision process. After displacement at 1.25 m, the force of the BL was below that of the other shell formulations. Nevertheless, considering typical fluctuations

and patterns, the results can be considered identical, with no significant discrepancy.

5.2 Strain and stress contours

Strain is indicated in nonlinear FEA when material and structural elements experience deformation, fracture, and finally destruction. The behavior of strain presented in Figure 6 represents an element on the upper side of the tearing length (outer shell) located in the impact region. The results indicate that the element had not fully experienced fracture as the ultimate strain was set to be 0.2. The BWC formulation produced final strain in the range of 0.075–0.1, which was also shared with the strain contour

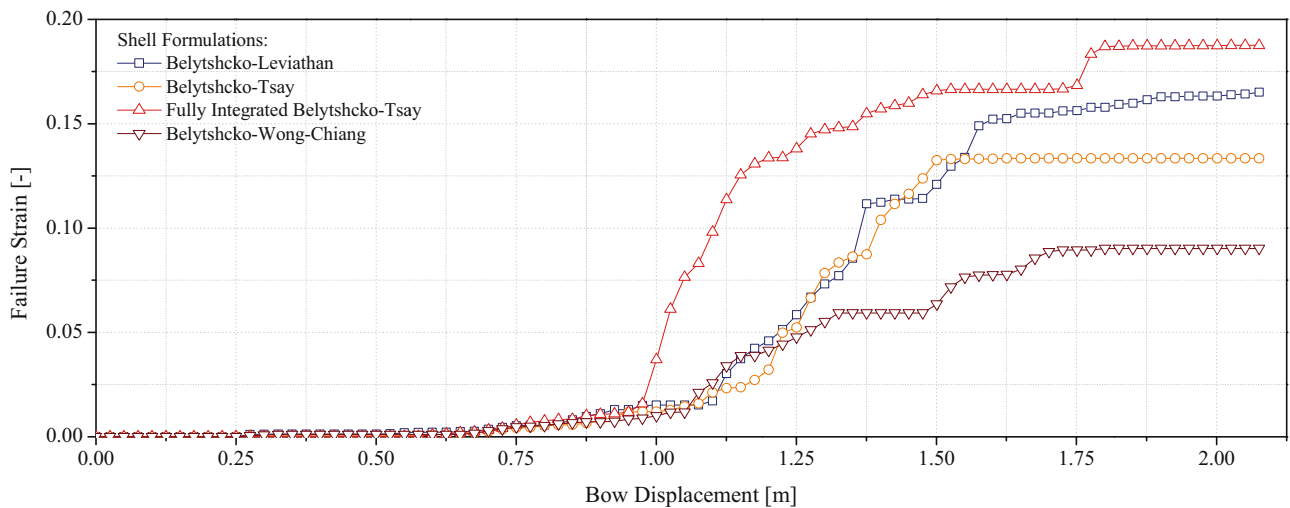


Figure 6: Behavior of failure strain on the side shell during impact.

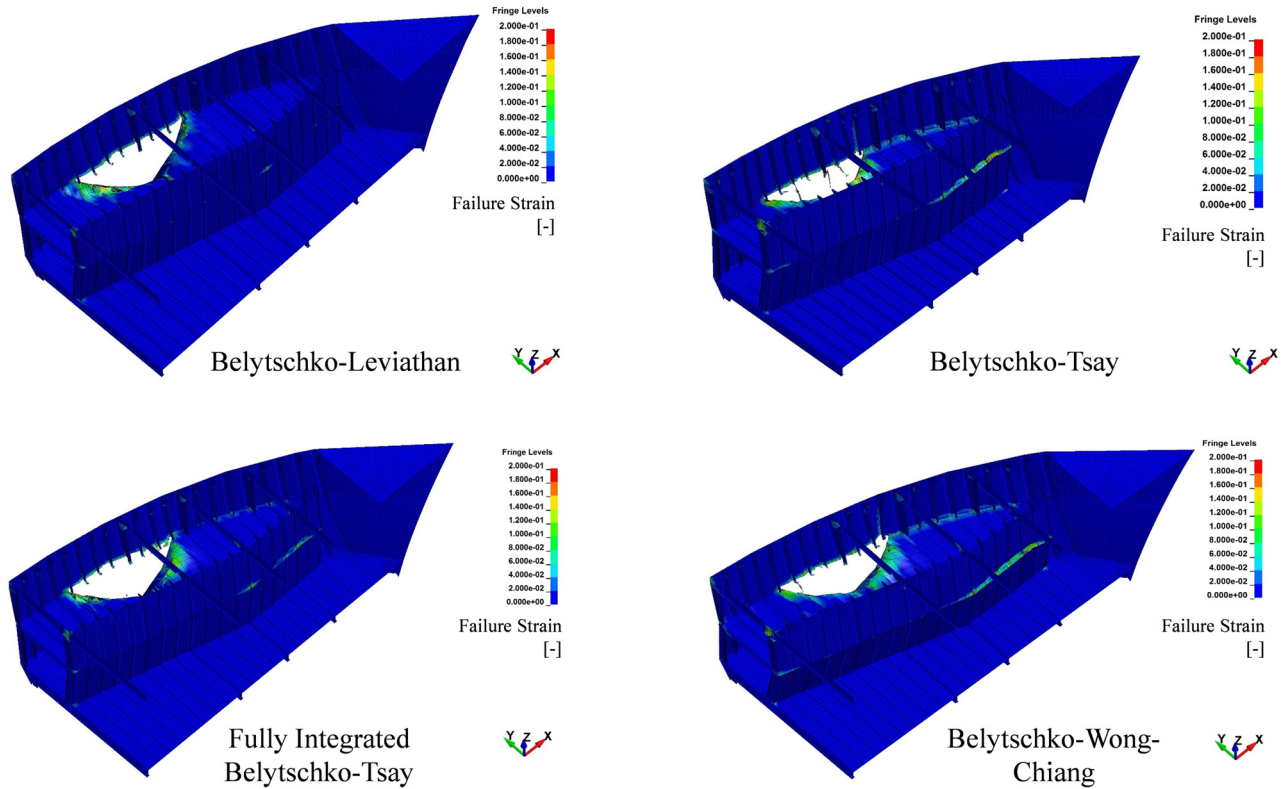


Figure 7: Failure strain of the selected shell EFs.

in the inner shell, as displayed in Figure 7. Interestingly, the mentioned formulation and the BT showed a longer strain contour, which indicates destroyed structures due to initial penetration on the outer shell lending more significance to the inner shell compared to the BL and the FI version of BT.

The similarity of the tendency of stress behavior (Figure 8) shows that the initial impact did not produce any fracture until

displacement at 0.25 m. Beyond this point, shell formulations tended to fluctuate in the same pattern until 1 m. The stress level experienced at the end of the calculation was highest with the BL formulation, while other formulations were reduced below 2×10^8 Pa. This phenomenon possibly occurs since the selected element may interact with other impacted members, and the latter causes higher fluctuation in stress history, while

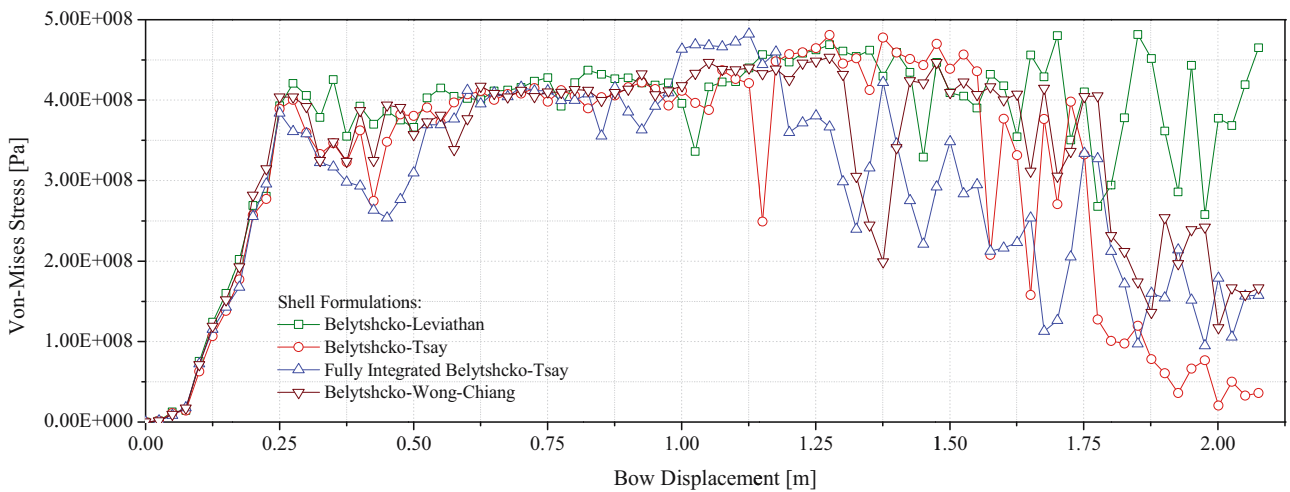


Figure 8: History of critical stress on the selected spot above the tearing damage on the side structure.

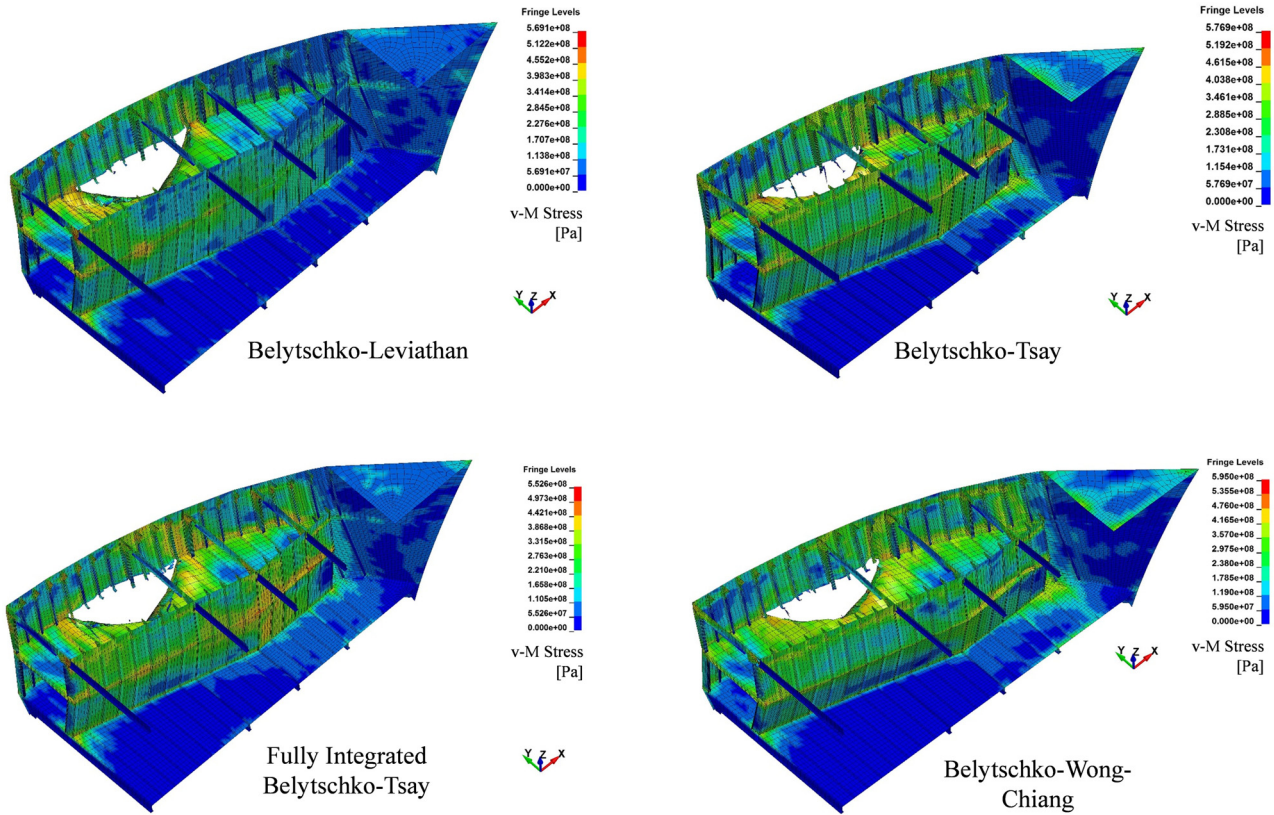


Figure 9: Critical stress contour of the target ship under ship collision.

a lower stress level indicates that beyond a certain bow displacement, the selected element on the side structures of the target ship was unaffected (or affected only at a low level) by the collision process. The comparison is more explicitly assessed at a global scale as presented in Figure 9, in which the longer strain contours of the BT and BWC formulations also appear as a longer stress contour with quite a high level on the inner shell, especially near the bow structure of the target ship.

5.3 Accumulated displacement

Displacement in this discussion refers to the component/member being displaced from its original position due to ship collision. The results in Table 4 are arranged by the displacement direction for each member, with the most displaced member during impact being the middle deck in the transversal direction at a range of 0.1577–0.3908 m. The car deck was found to be the least affected by impact

Table 4: Displacement of the involved member in ship collision

Direction	Member	Formulation			
		BL	BT	BT-FI	BWC
Longitudinal (m)	Middle deck	0.0484	0.1041	0.0631	0.1129
	Car deck	0.0003	0.0003	0.0003	0.0003
	Side shells	0.0251	0.0455	0.0351	0.0494
	Struct. frames	0.0193	0.0408	0.0269	0.0463
	Upper/main deck	0.0006	0.0011	0.0007	0.0016
Transversal (m)	Middle deck	0.1577	0.3510	0.3908	0.3908
	Car deck	0.0001	0.0002	0.0002	0.0002
	Side shells	0.0997	0.1629	0.1789	0.1789
	Struct. frames	0.0826	0.1521	0.1692	0.1692
	Upper/main deck	0.0005	0.0018	0.0027	0.0027
Vertical (m)	Middle deck	0.0569	0.0621	0.0220	0.0544
	Car deck	0.0075	0.0077	0.0058	0.0076
	Side shells	0.0107	0.0128	0.0107	0.0128
	Struct. frames	0.0052	0.0158	0.0051	0.0155
	Upper/main deck	0.0075	0.0218	0.0061	0.0380

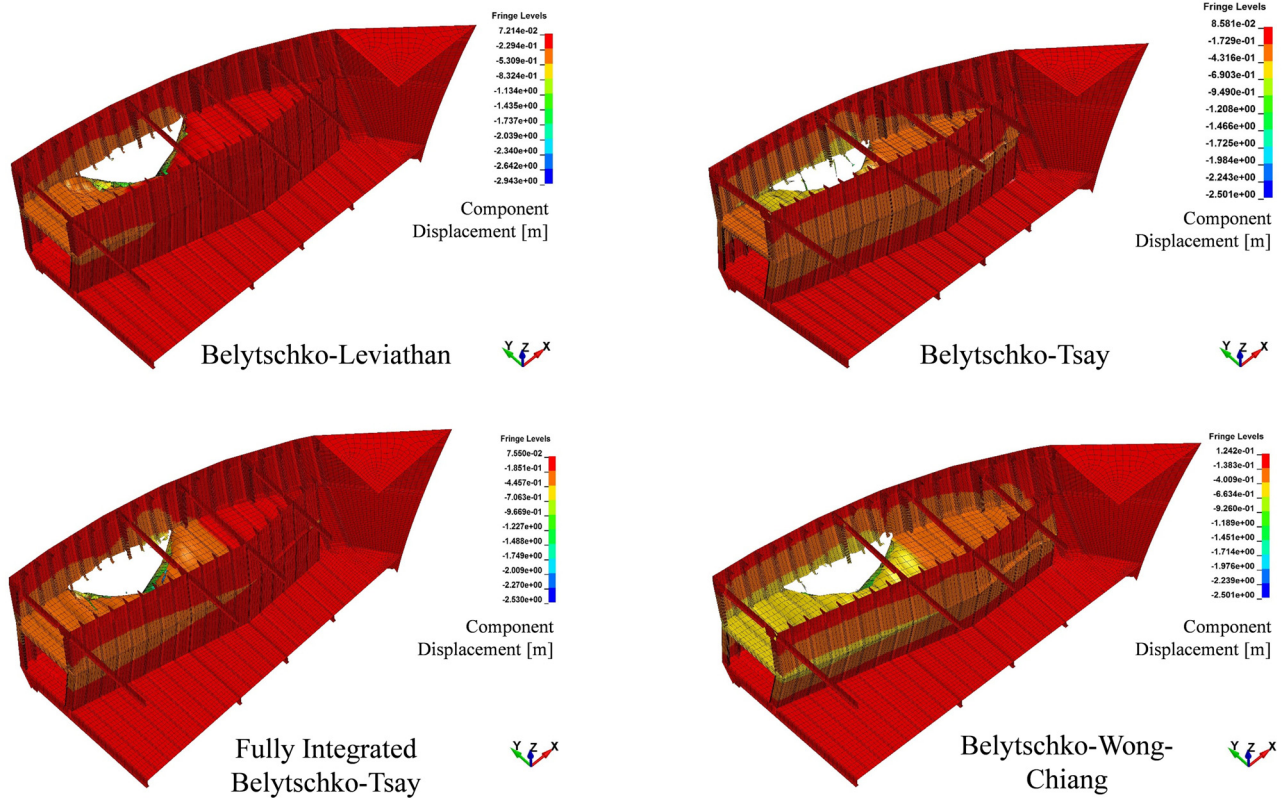


Figure 10: Displacement level of the side structure involved in ship collision.

as all formulations produced very similar results in terms of displacement to the longitudinal, transversal, and vertical directions. Nonlinearity was hardly observed for this member, which indicates that the crushing of other members did not significantly affect the position of this member. The overall results indicate that the displacement level of members produced by the BT, the FI version of BT, and the BWC formulations was the most similar; however, in the case of the structural frames, the BT and the BWC were very similar in terms of displacement in three directions. Nevertheless, quantifying the formulation effect in specific ways, *e.g.*, on member behavior, requires extensive observation due to the nonlinearity and dynamic characteristic of structures under impact loading.

As a solution, a larger-scale observation of the structural displacement contour was conducted as presented in Figure 10, which explicitly documents the behavior of two important members of the side structure, *i.e.*, the outer and inner shell. There was an indication of similarity in member behavior in terms of the overall contour for the BT and the BWC formulations, whereas a wide range of displacement on both shells was found from their produced results. The FI version of the BT actually shared an identical pattern with the BL, but the displacement on

the inner shell of the latter formulation was found to be very small. This identification process regarding the displacement behavior provides a good correlation with the energy response, for which the BL produced the lowest internal energy and total energy.

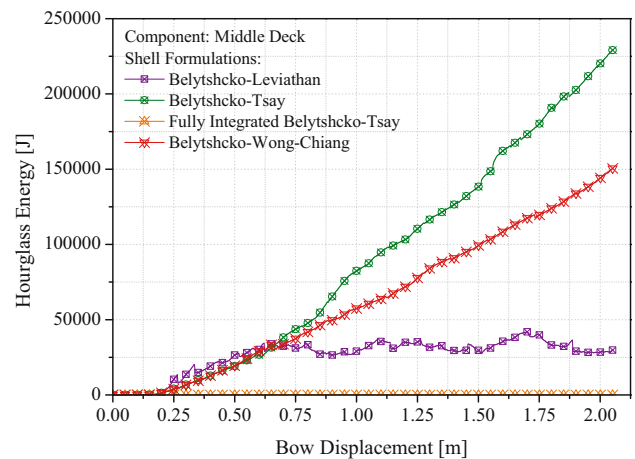


Figure 11: Hourglass pattern during collision of the local member: car deck.

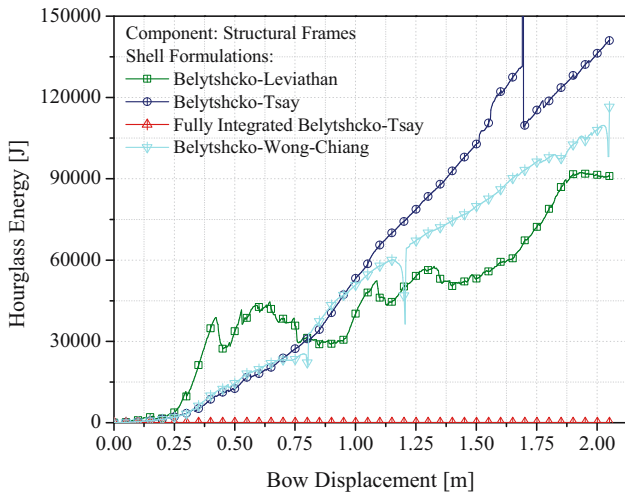


Figure 12: Hourglass pattern during collision of the local member: structural frames.

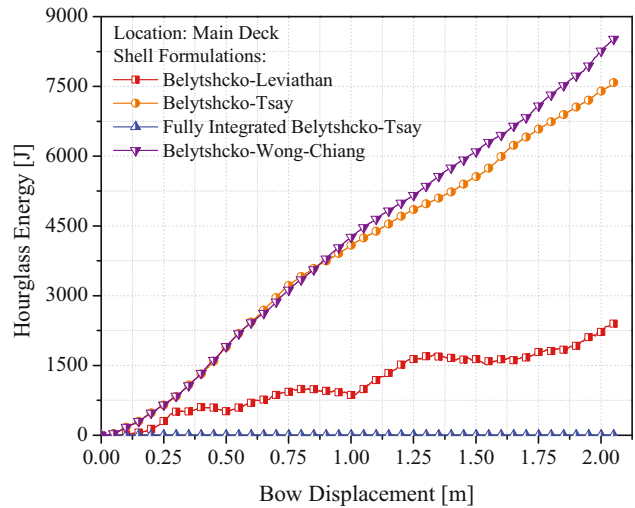


Figure 14: Hourglass pattern during collision of the local member: middle deck.

5.4 Hourglass behavior and time analysis

Hourglass modes are nonphysical, zero-energy modes of deformation that produce zero strain and no stress. Hourglass modes occur only in under-integrated (single integration point) solid, shell, and thick shell elements. This energy is undesired by researchers, especially in the NLFEA field, as it reduces the accuracy of calculations. To confirm that the nonphysical hourglass energy is small, the energy should be relatively small in comparison with the peak internal energy for each part/member – less than 10% as a rule of thumb [46].

An initial assessment of the global results from the previous section (referring to Table 3) leads us to conclude that only BL and FI BT produce very good results in terms of the

hourglass-to-internal-energy ratio, with values of 9.96 and 0%, consecutively. However, the hourglass assessment addresses each part of the structure, which produces calculation results for each member directly involved in impact loading. Figures 11–15 record the hourglass energy of the target ship during ship collision. The results suggest that all shell formulations are acceptable for NLFEA. This is also clear from the analysis of ships during collision, performed in previous studies and examined in considerable detail [49–54].

Another important parameter in FEA is time simulation, as described by Bathe [55]. There are also several considerations when performing the FEA: for instance, the mesh size selection [56–58] and failure criteria [59–62]. The

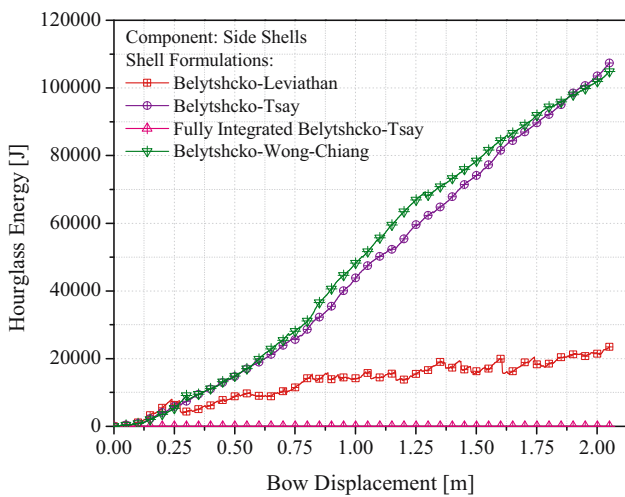


Figure 13: Hourglass pattern during collision of the local member: main deck.

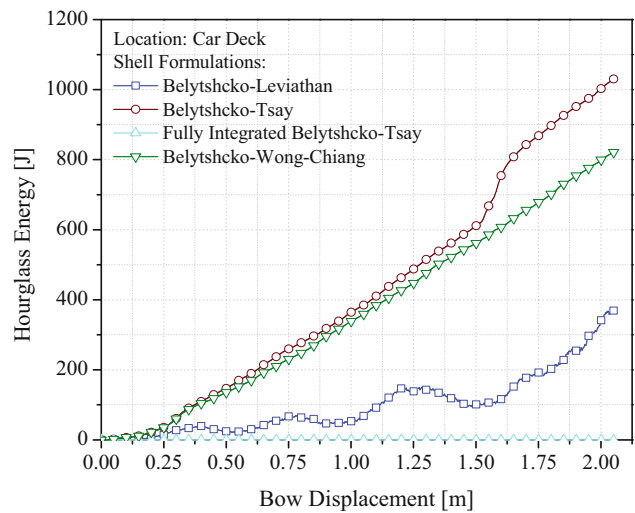


Figure 15: Hourglass pattern during collision of the local member: side shells.

Table 5: Time processing of the collision analysis

Information	BL	BT	BT-FI	BWC
CPU time per zone cycle (ns)	156	116	277	147
Problem cycle (cycle)	325,226	778,499	323,327	42,736
Total CPU time (s)	3,767	6,719	6,637	4,463

common material properties of steels used in FEA models can be found in the study conducted by Ridwan *et al.* [63]. Reliability and effectiveness are two different but related aspects to consider in FEA; reliability is an extension of accuracy, while effectiveness represents an acceptable time frame. Deploying a very fine mesh or FI version formulation is a way to ensure that this parameter is fulfilled. However, the time of a simulation can increase, and, in some cases, leads to an unacceptable processing time. On the other hand, a very coarse mesh or selection formulation with a rapid calculation ability may indeed have good effectiveness, but the accuracy of the results could be questionable [64–70]. Based on these formulations, processing time must be assessed as a follow-up of the previous discussion focused on the accuracy of results (reliability). Table 5 suggests that the fastest results were produced by the BL and BWC formulations. Two versions of (BT and BT-FI) produced the slowest results. Although the BL formulation has a good hourglass-to-internal-energy ratio, for an analysis involving more complex structures and arrangements, the FI-BT is still recommended as it is capable to ensure hourglass to be suppressed.

6 Conclusions

This work was addressed to assess the effect of shell EFs on structural crashworthiness in NLFEA. Calibration of the current FE methodology was conducted in the initial stage of this research by considering a pioneer impact test on a stiffened panel. The results indicated good similarity between the current results and the laboratory test. This was confirmed by a previous work that used FEA to simulate the same impact case to calibrate fracture behavior. Satisfactory results were achieved in this stage, with a mesh size of 15 mm of the current configuration producing the most similar results to the previous simulation.

Extended study was performed on a more complex structure, *i.e.*, a double-hull structure, with the objective of quantifying the effect of shell formulation on the structural response produced. With regard to energy, hourglass was proven to be entirely avoided by deploying the FI

version of BT, while the ratio of global energy indicated that the BL was also a viable formulation for NLFEA. A close correlation between the internal energy and stress-strain produced lower energy and caused a lesser stress level and smaller strain contours. Crushing force, on the other hand, showed homogeneity across all formulations, producing a result when major damage on the side structure had not occurred or was in the range of approximately 0–1 m. Based on the history of critical stress estimated by the two versions of BT and BWC, in the end, they produced stress reduction compared to the middle of the impact process, which indicated that the selected element was no longer mainly affected by the crushing process. For evaluating the hourglass energy, it was important to ensure a ratio of hourglass-to-internal energy per part of 10%. All formulations matched the criterion and were capable of being deployed as part of the structural configuration in NLFEA. Nevertheless, the FI-BT is highly recommended for use as a shell formulation since the ratio in the global scale had an hourglass value of zero. Moreover, in terms of reliability, time processing as part of effectiveness had to be assessed as a consideration in the NLFEA process. The BL formulation produced the fastest results, followed by the BWC. On the other hand, the FI BT required more processing time as compensation for the suppression of hourglass energy.

Calibration and benchmarking are important aspects in FEA, especially for analyzing highly dynamic and non-linear phenomena. Quantification of the formulation effect on the structural response at a very specific level, *i.e.*, structure members, is exhausting work, so a rapid estimation is recommended to consider the global response. As a future extension of this study, one might consider the effect of shell formulations in calculating major and minor collisions.

Funding information: This work was supported by the “Penelitian Fundamental – Reguler Program (Fundamental Research – Regular Program), Year 2023” in the Ministry of Education, Culture, Research, and Technology, Indonesia, under the main contract no. 160/E5/PG.02.00.PL/2023 and the derived contract no. 1280.1/UN27.22/PT.01.03/2023. The authors gratefully acknowledge the support.

Author contributions: All authors have accepted responsibility for the entire content of this manuscript and approved its submission.

Conflict of interest: The authors declare no conflicts of interest.

Data availability statement: The authors declare that the data supporting the findings of this study are available within the article.

References

- [1] Bulian G, Cardinale M, Francescutto A, Zaraphonitis G. Complementing SOLAS damage ship stability framework with a probabilistic description for the extent of collision damage below the waterline. *Ocean Eng.* 2019;186(May):106073.
- [2] Sèbe M, Kontovas CA, Pendleton L. A decision-making framework to reduce the risk of collisions between ships and whales. *Mar Policy.* 2019;109:103697.
- [3] Prabowo AR, Bae DM. Environmental risk of maritime territory subjected to accidental phenomena: Correlation of oil spill and ship grounding in the Exxon Valdez's case. *Results Eng.* 2019;4(Jul):100035.
- [4] Otto S, Pedersen PT, Samuelides M, Sames PC. Elements of risk analysis for collision and grounding of a RoRo passenger ferry. *Mar Struct.* 2002;15(4–5):461–74.
- [5] Zhang AM, Zeng LY, Cheng XD, Wang SP, Chen Y. The evaluation method of total damage to ship in underwater explosion. *Appl Ocean Res.* 2011;33(4):240–51.
- [6] Minorsky VU. An analysis of ship collision with reference to protection of nuclear power ships. *J Ship Res.* 1959;3(2):1–4.
- [7] Woisin G. Design against collision. *Schiff Hafen.* 1979;31(2):105969.
- [8] Vaughan H. The tearing strength of mild steel plate. *J Ship Res.* 1980;24(2):96–100.
- [9] Zhang S, Pedersen PT, Villavicencio R. Probability and mechanics of ship collision and grounding. Oxford, UK: Butterworth-Heinemann, Elsevier; 2019.
- [10] Tabri K, Broekhuijsen J, Matusiak J, Varsta P. Analytical modelling of ship collision based on full-scale experiments. *Mar Struct.* 2009;22(1):42–61.
- [11] Liu B, Guedes Soares C. Simplified analytical method for evaluating web girder crushing during ship collision and grounding. *Mar Struct.* 2015;42:71–94.
- [12] Calle MAG, Oshiro RE, Alves M. Ship collision and grounding: Scaled experiments and numerical analysis. *Int J Impact Eng.* 2017;103:195–210.
- [13] Ansori DTA, Prabowo AR, Muttaqie T, Muhayat N, Laksono FB, Tjahjana DDDP, et al. Investigation of honeycomb sandwich panel structure using aluminum alloy (AL6XN) material under blast loading. *Civ Eng J.* 2022;8(5):1046–68.
- [14] Gao Y, Hu Z, Ringsberg JW, Wang J. An elastic-plastic ice material model for ship-iceberg collision simulations. *Ocean Eng.* 2015;102:27–39.
- [15] Qiankun J, Gangyi D. A finite element analysis of ship sections subjected to underwater explosion. *Int J Impact Eng.* 2011;38(7):558–66.
- [16] AbuBakar A, Dow RS. The impact analysis characteristics of a ship's bow during collisions. *Eng Fail Anal.* 2019;100(Aug 2018):492–511.
- [17] Mubarak MAH, Prabowo AR, Muttaqie T, Muhayat N. Dynamic structural assessment of blast wall designs on military-based vehicle using explicit finite element approach. *Math Prob Eng.* 2022;2022:5883404.
- [18] Lin Y, Min J, Li Y, Lin J. A thin-walled structure with tailored properties for axial crushing. *Int J Mech Sci.* 2019;157–158:119–35.
- [19] Debski H. Numerical and experimental analysis of stability of thin-walled composite structures subjected to eccentric load. *Arch Civ Mech Eng.* 2019;19(3):792–802.
- [20] Fajri A, Prabowo AR, Muhayat N. Assessment of ship structure under fatigue loading: FE benchmarking and extended performance analysis. *Curved Layer Struct.* 2022;9(1):163–86.
- [21] Lopresto V, Langella A, Abrate S. Dynamic response and failure of composite materials and structures. Cambridge (MA), USA: Woodhead Publishing; 2017.
- [22] Katili I, Batoz JL, Maknun IJ, Hamdouni A, Millet O. The development of DKMQ plate bending element for thick to thin shell analysis based on the Naghdi/Reissner/Mindlin shell theory. *Finite Elem Anal Des.* 2015;100:12–27.
- [23] Ahmad S, Irons BM, Zienkiewicz OC. Analysis of thick and thin shell structures by curved finite elements. *Int J Numer Methods Eng.* 1970;2(3):419–51.
- [24] Schoop H. A simple nonlinear flat element for large displacement structures. *Comput Struct.* 1989;32(2):379–85.
- [25] Buechter N, Ramm E. Shell theory versus degeneration—a comparison in large rotation finite element analysis. *Int J Numer Methods Eng.* 1992;34(1):39–59.
- [26] Meek JL, Ristic S. Large displacement analysis of thin plates and shells using a flat facet finite element formulation. *Comput Methods Appl Mech Eng.* 1997;145(3–4):285–99.
- [27] Hassis HA. “warping” theory of plate deformation. *Eur J Mech A/ Solids.* 1998;17(5):843–53.
- [28] ANSYS. ANSYS LS-DYNA user's guide. Canonsburg (PA), USA: ANSYS, Inc; 2019.
- [29] ANSYS. ANSYS mechanical APDL element reference. Canonsburg (PA), USA: ANSYS, Inc; 2013.
- [30] Chen BQ, Liu B, Soares CG. Experimental and numerical investigation on the influence of stiffeners on the crushing resistance of web girders in ship grounding. *Mar Struct.* 2019;63:351–63.
- [31] Prabowo AR, Muttaqie T, Sohn JM, Bae DM. Nonlinear analysis of inter-island RoRo under impact: Effects of selected collision's parameters on the crashworthy double-side structures. *J Braz Soc Mech Sci Eng.* 2018;40:248.
- [32] Tornabene F, Viscoti M, Dimitri R, Reddy JN. Higher order theories for the vibration study of doubly-curved anisotropic shells with a variable thickness and isogeometric mapped geometry. *Compos Struct.* 2021;267(Feb):113829.
- [33] Tornabene F, Fantuzzi N, Bacciocchi M, Reddy JN. An equivalent layer-wise approach for the free vibration analysis of thick and thin laminated and sandwich shells. *Appl Sci.* 2017;7(1):17.
- [34] Milazzo A. Layer-wise and equivalent single layer models for smart multilayered plates. *Compos Part B Eng.* 2014;67:62–75.
- [35] Reddy JN. Energy principles and variational methods in applied mechanics. Hoboken (NJ), USA: John Wiley & Sons; 2017.
- [36] Alsos HS, Amdahl J. On the resistance to penetration of stiffened plates, Part I - Experiments. *Int J Impact Eng.* 2009;36(6):799–807.
- [37] Cerik BC, Lee K, Park SJ, Choung J. Simulation of ship collision and grounding damage using Hosford-Coulomb fracture model for shell elements. *Ocean Eng.* 2019;173(Jan):415–32.
- [38] Pack K, Tancogne-Dejean T, Gorji MB, Mohr D. Hosford-Coulomb ductile failure model for shell elements: Experimental identification and validation for DP980 steel and aluminum 6016-T4. *Int J Solids Struct.* 2018;151:214–32.
- [39] Gu G, Mohr D. Anisotropic Hosford-Coulomb fracture initiation model: Theory and application. *Eng Fract Mech.* 2015;147:480–97.

- [40] Gorji MB, Mohr D. Predicting shear fracture of aluminum 6016-T4 during deep drawing: Combining Yld-2000 plasticity with Hosford–Coulomb fracture model. *Int J Mech Sci.* 2018;137:105–20.
- [41] Prabowo AR, Tuswan T, Ridwan R. Advanced development of sensors' roles in maritime-based industry and research: From field monitoring to high-risk phenomenon measurement. *Appl Sci.* 2021;11(9):3954.
- [42] Wang JJ, Song YC, Wang W, Chen CJ. Evaluation of flexible floating anti-collision device subjected to ship impact using finite-element method. *Ocean Eng.* 2022;178:321–30.
- [43] Prabowo AR, Tuswan T, Prabowoputra DM, Ridwan R. Deformation of designed steel plates: An optimisation of the side hull structure using the finite element approach. *Open Eng.* 2021;11(1):1034–47.
- [44] Ren Y, Meng Q, Chen C, Hua X, Zhang Z, Chen Z. Dynamic behavior and damage analysis of a spar-type floating offshore wind turbine under ship collision. *Eng Struct.* 2022;272:114815.
- [45] Akbar MS, Prabowo AR, Tjahjana DDDP, Tuswan T. Analysis of plated-hull structure strength against hydrostatic and hydrodynamic loads: A case study of 600 TEU container ships. *J Mech Behav Mater.* 2021;30(1):237–48.
- [46] LS-DYNA. Hourglass. LS-DYNA Support. 2019. <https://www.dynasupport.com/howtos/element/hourglass>.
- [47] Ridwan R, Nuriana W, Prabowo AR. Energy absorption behaviors of designed metallic square tubes under axial loading: Experiment - based benchmarking and finite element calculation. *J Mech Behav Mater.* 2022;31(1):443–61.
- [48] Prabowo AR, Ridwan R, Muttaqie T. On the resistance to buckling loads of idealized hull structures: FE analysis on designed-stiffened plates. *Designs.* 2022;6(3):46.
- [49] Ridwan R, Prabowo AR, Muhayat N, Putranto T, Sohn JM. Tensile analysis and assessment of carbon and alloy steels using FE approach as an idealization of material fractures under collision and grounding. *Curved Layer Struct.* 2020;7(1):188–98.
- [50] Prabowo AR, Muttaqie T, Sohn JM, Harsritanto BIR. Investigation on structural component behaviours of double bottom arrangement under grounding accidents. *Theor Appl Mech Lett.* 2019;9(1):50–9.
- [51] Prabowo AR, Bae DM, Sohn JM. Comparing structural casualties of the Ro-Ro vessel using straight and oblique collision incidents on the car deck. *J Mar Sci Eng.* 2019;7(6):183.
- [52] Cao B, Bae D-M, Sohn J-M, Prabowo AR, Chen TH, Li H. Numerical Analysis for Damage Characteristics Caused By Ice. *ASME 2016 35th International Conference on Ocean, Offshore and Arctic Engineering*; 2016 Jun 19–24; Busan, South Korea. ASME, 2016.
- [53] Prabowo AR, Bae DM, Sohn JM, Zakki AF, Cao B, Wang Q. Analysis of structural damage on the struck ship under side collision scenario. *Alex Eng J.* 2018;57(3):1761–71.
- [54] Prabowo AR, Byeon JH, Cho HJ, Sohn JM, Bae DM, Cho JH. Impact phenomena assessment: Part I-Structural performance of a tanker subjected to ship grounding at the Arctic. *MATEC Web Conf.* 2018;159:02061.
- [55] Bathe KJ. *Finite element procedures.* Upper Saddle River (NJ), USA: Prentice Hall; 2006.
- [56] Kuznecovs A, Schreuder M, Ringsberg JW. Methodology for the simulation of a ship's damage stability and ultimate strength conditions following a collision. *Mar Struct.* 2021;79:103027.
- [57] Alwan FHA, Prabowo AR, Muttaqie T, Muhayat N, Ridwan R, Laksono FB. Assessment of ballistic impact damage on aluminum and magnesium alloys against high velocity bullets by dynamic FE simulations. *J Mech Behav Mater.* 2022;31(1):595–616.
- [58] Dzulfiqar MF, Prabowo AR, Ridwan R, Nubli H. Assessment on the designed structural frame of the automatic thickness checking machine - Numerical validation in FE method. *Procedia Struct Integr.* 2021;33(C):59–66.
- [59] AbuBakar A, Dow RS. Simulation of ship grounding damage using the finite element method. *Int J Sol Struct.* 2013;50(1):623–36.
- [60] Prabowo AR, Ridwan R, Tuswan T, Imaduddin F. Forecasting the effects of failure criteria in assessing ship structural damage modes. *Civ Eng J.* 2022;8(10):2053–68.
- [61] Carvalho H, Ridwan R, Sudarno S, Prabowo AR, Bae DM, Huda N. Failure criteria in crashworthiness analysis of ship collision and grounding using FEA: Milestone and development. *Mek Maj Ilm Mek.* 2023;22(1):30–9.
- [62] Prabowo AR, Ridwan R, Tuswan T, Sohn JM, Surojo E, Imaduddin F. Effect of the selected parameters in idealizing material failures under tensile loads: Benchmarks for damage analysis on thin-walled structures. *Curved Layer Struct.* 2022;9(1):258–85.
- [63] RidwanPutranto T, Laksono FB, Prabowo AR. Fracture and damage to the material accounting for transportation crash and accident. *Procedia Struct Integr.* 2020;27(2020):38–45.
- [64] Faqih I, Adiputra R, Prabowo AR, Muhayat N, Ehlers S, Braun M. Hull girder ultimate strength of bulk carrier (HGUS-BC) evaluation: Structural performances subjected to true inclination conditions of stiffened panel members. *Results Eng.* 2023;18:101076.
- [65] Suryanto S, Prabowo AR, Muttaqie T, Istanto I, Adiputra R, et al. Evaluation of high-tensile steel using nonlinear analysis: Experiment-FE materials benchmarking of LNG carrier structures under low-temperature conditions. *Energy Rep.* 2023;9(Suppl 9):149–61.
- [66] Satriawan CYG, Prabowo AR, Muttaqie T, Ridwan R, Muhayat N, Carvalho H, et al. Assessment of the beam configuration effects on designed beam-column connection structures using FE methodology based on experimental benchmarking. *J Mech Behav Mater.* 2023;32(1):20220284.
- [67] Lutfi YM, Adiputra R, Prabowo AR, Utsunomiya T, Erwandi E, Muhayat N. Assessment of the stiffened panel performance in the OTEC seawater tank design: Parametric study and sensitivity analysis. *Theor Appl Mech Lett.* 2023;13(4):100452.
- [68] Do QT, Muttaqie T, Nhut P-T, Vu MT, Khoa ND, Prabowo AR. Residual ultimate strength assessment of submarine pressure hull under dynamic ship collision. *Ocean Eng.* 2022;266:112951.
- [69] Prabowo AR, Baek SJ, Cho HJ, Byeon JH, Bae DM, Sohn JM. The effectiveness of thin-walled hull structures against collision impact. *Lat Am J Solid Struct.* 2017;14(7):1345–60.
- [70] Yusvika M, Prabowo AR, Tjahjana DDDP, Sohn JM. Cavitation prediction of ship propeller based on temperature and fluid properties of water. *J Mar Sci Eng.* 2020;8(6):465.